PARTEC 95
International Congress for Particle Technology
11th European Conference of ILASS-Europe
on Atomization and Sprays
21. - 23. March 1995
Nürnberg, Germany

K.- P. Schade (Speaker)**, T. Frank, T. Hädrich and D. Petrak**

Technische Universität Chemnitz-Zwickau
Lehrstuhl Technische Thermodynamik/Wärmelehre
D 09107 Chemnitz, Germany

An Experimental and Numerical Study of the Two Phase Flows in Sprays with Hollow Cone Nozzles and Full Cone Nozzles

1 Introduction

The process of impulse, heat and mass transfer between a continuous and dispersed phase is involved in many spray processes e.g. in a smoke gas scrubber or in a spray drier. The advantage of a spray is the large specific surface of contacting liquids and gases. The aerodynamic behaviour of sprays is very complex and researcher have investigated gas entrainment using single atomisers /1/ and multiple atomisers /2/. The micro behaviour of drops such as the radial distributions of the dropsize, velocity and volume flux was determined to clarify the general spray structure by phase Doppler particle analyzer. /3/. Another interesting point are the aerodynamics of a spray in a gas flow as a gas scrubber with a vertically downward directed nozzle spray and a countercurrent gas flow. Gruß /4/ has predicted the gas flow field around a spray in a spray column. The spray was generated by a full cone nozzle and the gas flow was homogeneous at the entrance cross section. The spray acts as an obstacle and the gas flow goes to the wall region of the column. Smoke gas scrubbers need however a uniform gas flow field over the spray field length.

At the Technische Universität Chemnitz-Zwickau, Forschungsgruppe Mehrphasenströmungen, the gas flow in a spray column has been investigated with a modified Laser Doppler technique. In addition the two phase flow has been calculated on the base of the Euler-Lagrange model. This work examines the flow field around a spray which was generated by a full cone nozzle and a hollow cone nozzle.

2 Test Facility and Measurements

2.1 Measurement Apparatus and Experimental Conditions

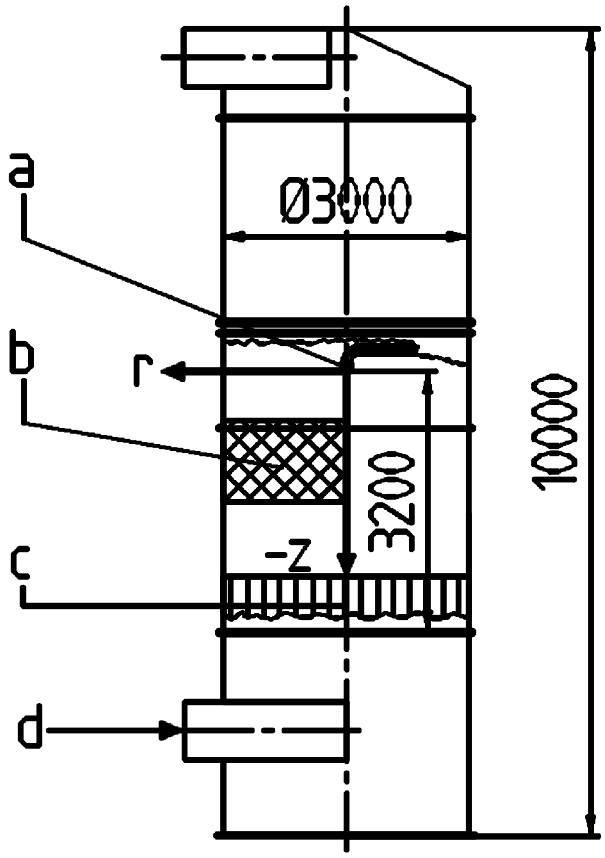

Figure 1. Experimental apparatus
a) nozzle b) meas. area
c) flow rectif. d) air input

The experiments were carried out in the spray column shown in figure 1. The spray column has a height of 10 m and the diameter of the circular cross section is 3 m. At the entrance cross section of the drop field the upward directed air flow is uniform with a disturbance of less than 10 %. The uniform air velocity profile across the column was realized by means of a system of a flow rectifier and two hole sheets. The maximum air velocity is 4 m/s.

The nozzle was arranged at the column symmetry axis in an upward distance of 3 m from the air entrance section and the spray of a full cone nozzle or a hollow cone nozzle is directed vertically downwards. We used nozzles of the Lechler company with the following characteristics:

- Full cone nozzle

axial-flow full cone nozzle	: type 403.566
volume flow rate (p = 100 kPa)	: 36.4 m³/h
spray angle	: 90°
Sauter mean diameter	: 1873 µm
arithmetic mean diameter	: 876.5 µm

- Hollow cone nozzle

hollow cone nozzle	: type AV-300.114.6D
volume flow rate (p = 100 kPa)	: 40 m³/h
spray angle	: 90°
Sauter mean diameter	: 1732 µm
arithmetic mean diameter	: 356.7 µm

The local velocity measurements of both the gas-phase and the droplet-phase were performed with a single-component laser Doppler velocimeter (LDV). There were measured only the streamwise velocity components u_F and u_P in z-direction parallel to the column-axis (fig.1). All experimental examinations were carried out under the following conditions:

- mean streamwise column gas velocity : $\bar{u}_M = 3$ m/s
- nozzle pressure : $p_N = 100$ kPa

The LDV was a semiconductor-LDV which works in backscattering mode. Since the original measuring head was not suitable for the direct use in a water spray, it was covered in a special protection case to disable the entering of water /5/.

In a distance of 0.5 m above and below the LDV measurement-point three small nozzles are mounted respectively. They spray mist droplets with an arithmetic mean diameter of about 10 µm perpendicular to the main gas stream in to the measurement volume.

2.2 Measurement Technique

The aim of the experimental investigations was the measurement of streamwise gas velocity in presence of water drops in a spray column. In order to trace gas velocity under these conditions mist droplets of about 10 µm diameter are required. The slip velocity of these mist droplets is about 0.003 m/s. Therefore the range of particle diameters inside the spray column is very large from 10 µm of mist droplets to 2000 µm of water drops from the scrubber nozzle. Up to now a phase Doppler device is unable to measure this wide diameter range simultaneously.

The idea to measure gas velocity with an usual laser Doppler velocimeter is the adding of water mist. At every location inside the spray column at first a measurement of only drop velocity was done without mist and a second with mist, thus recording both drop and gas velocities. These measurements were done under same conditions and over an equal measuring period. In order to acquire probably equal number of drops in both measurements the data rate must be much lower than the maximum data rate of the recording system i.e. neglectable data losses. The calculation of gas velocity from measured drop and drop with mist velocities is as follows.

Because an acquired data in the second measurement can only arise from a water drop or a mist droplet the following equations are valid:

$$n_{P+F} = n_P + n_F \tag{1}$$

$$\sum u_{P+F} = \sum u_P + \sum u_F \tag{2}$$

$$\sum u_{P+F}^2 = \sum u_P^2 + \sum u_F^2 \tag{3}$$

The statistic values of the gas velocity may be calculated using (1 .. 3) with:

$$\bar{u}_F = \frac{\sum u_F}{n_F} = \frac{\sum u_{P+F} - \sum u_P}{n_{P+F} - n_P} \tag{4}$$

$$\sigma^2(u_F) = \frac{\sum u_F^2}{n_F} - \bar{u}_F^2 = \frac{\sum u_{P+F}^2 - \sum u_P^2}{n_{P+F} - n_P} - \bar{u}_F^2 \tag{5}$$

In order to get sufficiently exact results with the equation (4) the relation $n_F > n_p$ has to be satisfied. The exactness of equation (5) depends strongly on the high variance of u_P so that $n_F >> n_p$ is required.

3 Numerical Prediction of the Gas-Droplet Flow

For the numerical prediction of the gas-droplet flow around a full cone and a hollow cone nozzle a modified version of the Navier-Stokes solver FAN-2D developed by Peric and Lilek /6/ was used. In order to account for the interaction effects between the gaseous and the droplet phase a Lagrangian stochastic-deterministic (LSD) model and the appropriate momentum exchange terms were incorporated into the numerical algorithm.

3.1 Equations of fluid motion

The motion of the gas-droplet flow was assumed to be radial symmetric and was calculated in the same cylindrical coordinate system (r, z) as described above.Further, the turbulent two-phase (gas-droplet) flow under consideration is described by assuming that the particulate phase is dilute, but the particle loading is appreciable. Interparticle effects are neglected, but the effects of the particles to the gas flow are taken into account. The two-phase flow is statistically stationary, incompressible and isothermal. The gas phase has constant physical properties and is Newtonian. Under these assumptions the time-averaged form of the governing gas-phase equations can be written in the following form of the general transport equation:

$$\frac{\partial}{\partial z}(\rho_F u_F \Phi) + \frac{1}{r}\frac{\partial}{\partial r}(r\rho_F v_F \Phi) = \frac{\partial}{\partial z}\left(\Gamma \frac{\partial \Phi}{\partial z}\right) + \frac{1}{r}\frac{\partial}{\partial r}\left(r\Gamma \frac{\partial \Phi}{\partial r}\right) + S_\Phi + S_\Phi^P \tag{6}$$

where Φ stands for u_F, v_F, k and ε. The terms S_Φ and Γ represent the "source" and the effective diffusion coefficient, respectivly and S_Φ^P represents the coupling between the gaseous and the droplet phase due to the particle-fluid interaction. This last term is calculated by solving the Lagrangian equations of droplet motion. The continuity equation is obtained by setting Φ=1, Γ=0. For modeling of fluid turbulence the standard k-ε turbulence model together with isotropic eddy viscosity and standard model constants are used /7/.

The influence of the droplet motion on fluid turbulence characteristics was neglected ($S_k^P = S_\varepsilon^P = 0$). The momentum source terms S_u^P and S_v^P in the Navier-Stokes equations

were calculated using the Particle-Source-in (PSI)-cell model developed by Crowe et al. /8/, /9/. In the PSI-cell model the force excerted on a fluid control volume by a single particle or droplet is calculated from the residence time of a particle in the control volume and the change in particle momentum in this time. In order to calculate the particle momentum source terms S_u^P and S_v^P in the momentum equations these points of intersection of the particle trajectory with the faces of the control volume have to be calculated and the particle and fluid properties have to be interpolated in there points. The particle momentum source term is then as follows :

$$S_u^P = \sum \dot{N}_P \rho_F \frac{A_P}{2} \int_{t_{in}}^{t_{out}} C_D v_{rel} (u_F - u_P) dt \qquad (7)$$

where the sum is taken over all the representative particles crossing the control volume. Because the number of test particles used for simulation is limited and different from that of particles or droplets which would actually cross the control volume, $\dot{N}_P$ characterises the droplet flow rate for a calculated representative particle trajectory.

3.2 Eqations of droplet motion

The droplet phase was treated by the Lagrangian approach where a large number of droplets were followed in time along their trajectories through the flow domain. Each droplet trajectory is associated with a droplet flow rate $\dot{N}_P$ and so represents a number of real droplets with the same physical properties. This representation is used in order to allow the consideration of the droplet size distribution and to simulate the appropriate liquid mass flow rate at the injection locations. The droplet trajectories were determined by solving the ordinary differential equations for the droplet location and velocity components. For the formulation of the droplets equation of motion it was assumed that the forces due to droplet rotation, the pressure gradient in the flow, added mass force and the Basset history term are negligible since a large density ratio ρ_P / ρ_F is considered. The equations of droplet motion can be written than as follows

$$\frac{d}{dt}\begin{bmatrix} z_P \\ r_P \end{bmatrix} = \begin{bmatrix} u_P \\ v_P \end{bmatrix}$$

$$\frac{d}{dt}\begin{bmatrix} u_P \\ v_P \end{bmatrix} = \frac{3}{4}\frac{\nu_F \rho_F}{\rho_P d_P^2} Re_P \, C_D(Re_P) \begin{bmatrix} u_F - u_P \\ v_F - v_P \end{bmatrix} + \frac{\rho_P - \rho_F}{\rho_P} \begin{bmatrix} -g \\ 0 \end{bmatrix} \qquad (8)$$

with :

$$Re_P = \frac{d_P v_{rel}}{\nu} \quad , \quad v_{rel} = \sqrt{(u_F - u_P)^2 + (v_F - v_P)^2} \qquad (9)$$

The drag coefficient C_D is calculated as a function of the particle Reynolds number using the correlations obtained by Morsi and Alexander /10/. The effect of turbulence

of the gas flow on the droplet motion was modeled by a stochastic procedure, the so called Lagrangian stochastic-deterministic (LSD) turbulence model. This model was proposed by Milojevic /11/, Schönung /12/ and other authers. The LSD turbulence model takes into account the instanteanous gas velocities calculated from the mean gas velocities u_F, v_F and from fluctuation velocities u_F', v_F'. The mean gas velocities were obtained from the solution of the Navier-Stokes equations but the values of the fluctuation velocities are sampled as random values in dependence on the local turbulence characteristics of the gaseous phase.

The boundary conditions for the droplet tracking procedure are specified as follows. Trajectories are calculated throughout the flow domain until the droplet leaves the flow domain through an inlet or outlet cross section. Droplets leaving the computational domain at the symmetry line (r=0) are replaced by droplets entering the domain with opposite radial velocity. For the droplet-wall interaction simple reflection with a restitution coefficient of 0.5 was assumed in the present calculations.

3.3 Solution procedure

The above equations of fluid motion were solved with the FAN-2D Navier-Stokes solver developed by Peric and Lilek /6/. The original algorithm was extended by introduction of the momentum source terms in the momentum equations of fluid motion. Efficiency of the solution method was ensured by applying an optimized underrelaxation technique not only to the fluid variables but also to the additional source terms. The equations of droplet motion were solved using a standard Runge-Kutta solution scheme of 4th order accuracy with automatic time step correction. In order to ensure sufficient resolution of the influence of fluid flow turbulence on the droplet motion the time step Δt was limited to a maximum of 1/10 the Lagrangian time scale T_L of the turbulent eddies.

The numerical procedure to obtain a converged solution for both phases is then as follows :

1. A converged solution of the gas flow field was calculated without source terms of the dispersed phase.
2. A large number of droplets were traced through the flow field and the values of the source terms were calculated for all control volumes of the numerical grid.
3. The flow field was recalculated by considering the source terms of the dispersed phase, were appropriate underrelaxation factors were considered.
4. Repetition of steps 2 and 3 until convergence was achieved.

The calculations were performed on a HP 735/755 workstation cluster. The performance of the droplet trajectory calculations could significantly be increased by EXPRESS based parallelization of the Lagrangian solver as described in more detail in /13/.

4 Results and Discussion

Figures 2 and 3 show the measured and calculated gas and droplet velocities for the hollow and the full cone nozzle in comparison. In figure 2 the velocitiy profiles of the gas-droplet flow around a full cone nozzle are plotted against the column radius in depence on the z-distance from the nozzle. The profiles of the calculated gas velocities are in reasonable agreement with the measured profiles in a distance from 1.2 m and 1.6 m downwards to the nozzle. The plots for z = -0.6 m and z = -0.8 m show measured values only for the range outside the spray cone. They are in good agreement with the calculated values. In the area of the spray cone and the spray cone border the condition $n_F > n_P$ not satisfied and so in accordance to equation (4) values for the gas velocity could not be obtained. It is not clear whether the mist droplets were washed out by the water nozzle droplets or blown away from the measurement point. Further investigations will clarify this problem.

The calculated velocities show the expected negative values in the spray cone and the increase of the velocity in the outer column region. The steep particle velocity increase markes the position of the spray cone border. In connection with the development of the gas velocity distribution the displacment of the gas flow to the outer column region is clear to see. The measurements show a large difference between the measured and the calculated droplet velocities. The reason is the different sensitivity to the particle size of the measuring and numerical technique. The used LDV collected the velocities from droplets with a diameter from 100 µm up to 2000 µm. In the real spray process besides the primary droplet production in the nozzle secondary droplets are produced by droplet-droplet, droplet-wall interactions and air-water interactions. These processes of droplet degradation and formation of a large number of small secondary droplets within the flow domain was not taken into account in the numerical calculations. The measuring of the obviously large number of smaller secondary droplets leads to the deviations.

In figur 3 the corresponding velocity profiles for the hollow cone nozzle are illustrated. First of all the air velocity profiles at all z-sections are rather uniform over the cross section. That means a hollow cone nozzle doesn´t displace the air stream outside the central region of the column as a full cone nozzle does. The agreement between measurement and calculation is also quite good. The variations in the measured gas velocity profiles comes from the support constructions at the column bottom. The deviation between the measured and the calculated particle velocity is similar to the deviation for the full cone measurement and is caused by the same effect. For the particle measurement near the nozzle, the primary droplets are dominant and the agreement with the calculation is better. But near the column bottom the influence of the secondary droplets is dominant and leads to greater differences.

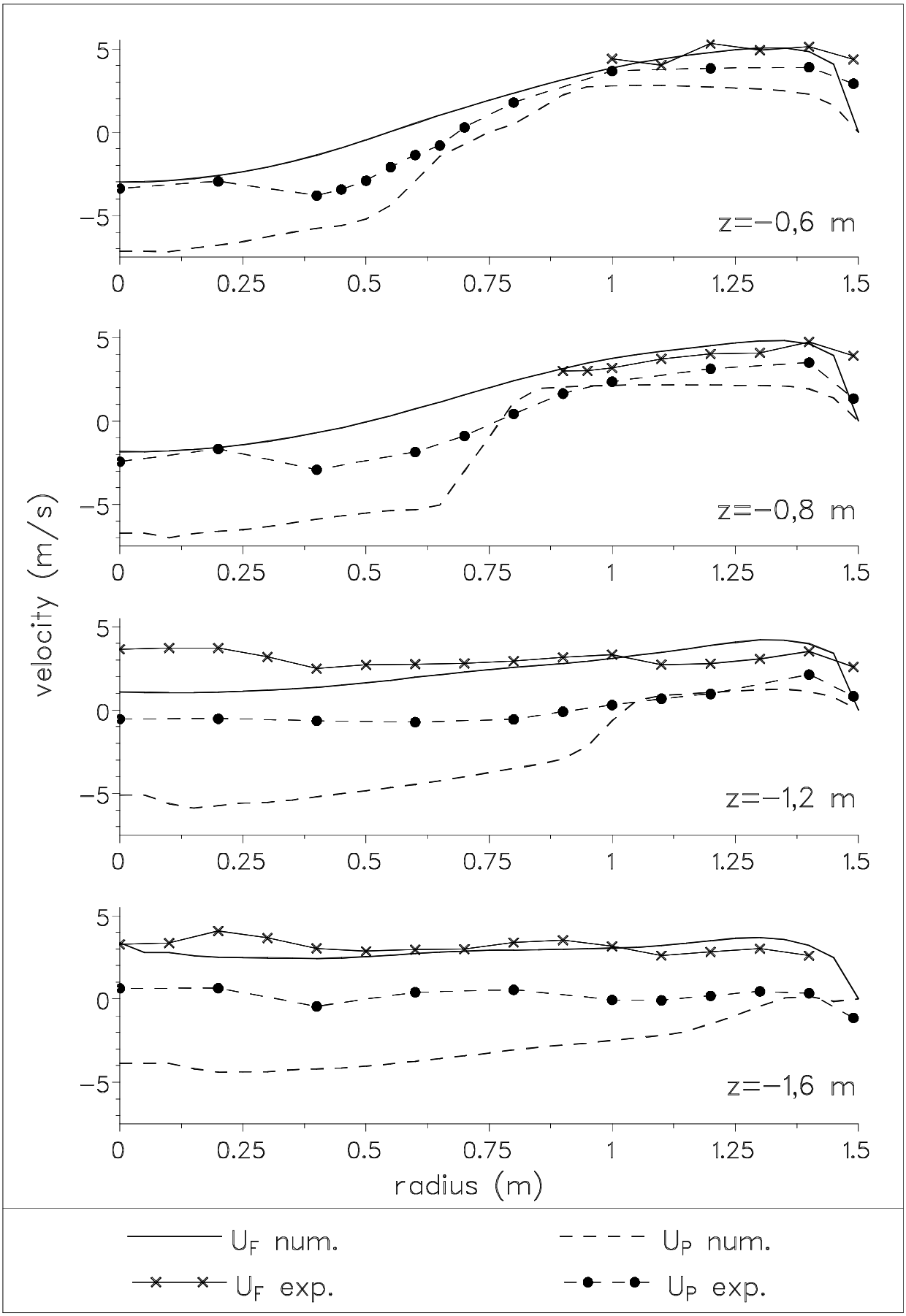

Figure 2 : Velocity profiles of the full cone nozzle

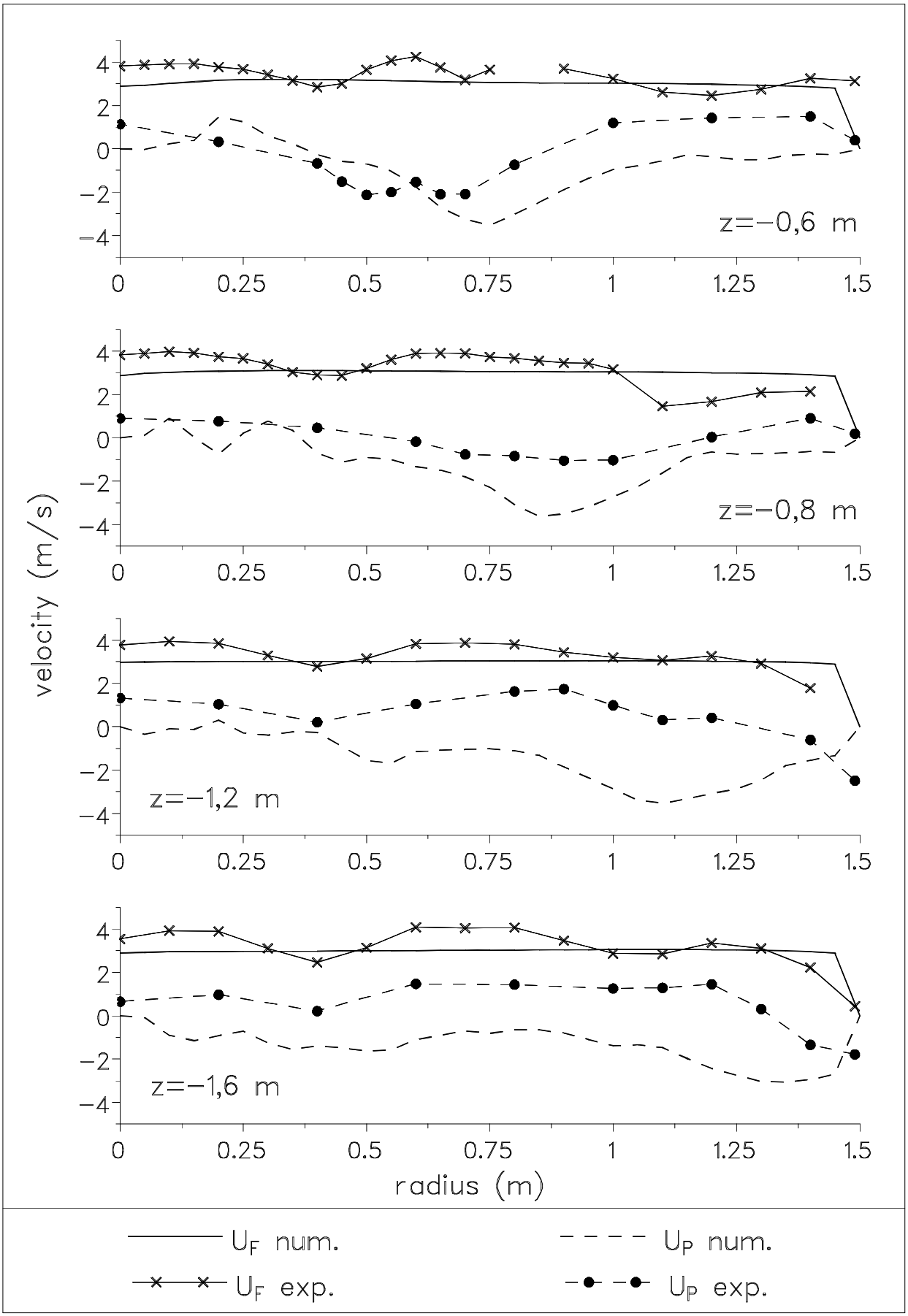

Figure 3 : Velocity profiles of the hollow cone nozzle

5 Summary

It has been found that the modified LDA system with the additional tracer droplet technique is suitable for measurements of the gas velocity in a gas-droplet two-phase flow of a spray column with a single nozzle and an uniform countercurrent gas velocity of 3 m/s in the entrance section. The radial gas velocity profile of the axial component over the spray length of a single hollow cone nozzle is quite uniform. For the full cone nozzle the uniform gas velocity profiles exist only in the lower spray sections. Near to the full cone nozzle the gas flow goes to the radial outer part of the column and has there greater velocity values.

Relating to the gas velocity the experimental results are in good agreement with the numerical velocity values for both nozzle types. Differences between the experimental and numerical results were established for the averaged droplet velocities because the considered droplet size distributions are different for the numerical predictions and the laser Doppler velocimeter measurements.

6 References

/1/ F. E. J. Briffa, N.Dombrowski — Entrainment of Air into a Liquid Spray.A. I. Ch. E. Journal 12(1966)708.

/2/ N. Dombrowski, J. Singh — An Experimental Study of Air Entrainment by Multiple Spray Nozzles. Proceedings of the ICLASS-91 Gaithersburg, MD, USA(1991)189-196.

/3/ N. Tokuoka, Y. Yamaguchi, M. Takada, F. Zhang — The Spray Structure from Swirl Atomizers. Proceedings of the ICLASS-91 Gaithersburg, MD, USA(1991)233-240.

/4/ J. Gruß — Numerische Simulation der Zweiphasenströmung Gas-Flüssigkeitstropfen im Sprühturm, Dissertation(1993) RWTH Aachen.

/5/ R. Schulze, Th. Hädrich , D. Petrak, G. Trommer — Geschwindigkeitsmessungen in einem Sprühturm mit einem Halbleiter Laser Velocimeter. Proceedings of 2. Fachtagung Lasermethoden in der Strömungsmeßtechnik, Braunschweig (1993), Verlag Shaker, 15.1-15.5.

/6/	M. Peric, Z. Lilek	User Manual for the FAN-2D Software Package for the Calculation of Incompressible Flows", 1993, Institut für Schiffbau der Universität Hamburg.
/7/	M. Peric	A Finite Volume Multigrid Method for Calculating Turbulent Flows, Proc. 7th Symposium on Turbulent Shear Flows, 1989, Vol. 1, pp. 7.3.1.-7.3.6., Stanford University, USA.
/8/	C.T. Crowe, M. P. Sharma D. E. Stock	The Particle-Source-In Cell (PSI-Cell) Model for Gas-Droplet Flows. Trans. of ASME, J. Fluids Eng., 1977, Vol. 99, pp. 325-332.
/9/	C.T. Crowe	REVIEW - Numerical Models for Dilute Gas-Particle Flows, Trans. of ASME, J. Fluids Eng., 1982, Vol. 104, pp. 297-303.
/10/	S.A. Morsi, A.J. Alexander	An Investigation of Particle Trajectories in Two-Phase Flow Systems, J. Fluid Mech., 1972, Vol. 55, part2, pp. 193-208.
/11/	D. Milojevic	Lagrangian Stochastic-Deterministic (LSD) Predictions of Particle Dispersion in Turbulence", Part. Part. Syst, Charact., 1990, Vol. 7, pp. 181-190.
/12/	B. Schönung	Comparison of Different Dispersion Models for Particles in Lagrangian and Eulerian Prediction Codes", 1987, In: Proc. of the Int. Conf. on Fluid Mech., Peking, July 1.-4. 1987, Peking University Press, China.
/13/	Th. Frank, I.Schulze	Numerical Simulation of Gas-Droplet Flow around a Nozzle in a Cylindrical Chamber using a Lagrangian Model based on a Multigrid Navier-Stokes Solver, 1994, Int. Symp. on Numerical Methods for Multiphase Flows, ASME Fluids Eng. Division, June 19.-23., Lake Tahoe, NV, USA.

7 Nomenclature

- n - number
- u_M - mean velocity
- σ^2 - variance of velocities
- A_p - cross sectional area of a droplet
- C_D - drag coefficient
- d_p - droplet diameter

ε - dissipation of turbulent kinetic energy
Γ - effective diffusion coefficient of the Φ transport equation
g - gravitational constant
k - turbulent kinetic energy
ν_F - kinematic viscosity
$\dot{N}_P$ - droplet flow rate for a representative droplet trajectory
Re_P - particle Reynolds number
ρ - density
r, z - coordinates shown in fig. 1
S_Φ - source term of the Φ transport equation
S_Φ^P - source term of the Φ transport equation due to interaction with the dropletphase
u, v - velocity components in axial and radial direction
u_F', v_F' - fluctuation velocities of the gaseous phase
v_{rel} - drift velocity between gas and droplets

7.1 Subscript or Superscript

F - properties of the fluid phase
P - properties of the droplet phase
P+F - properties of the droplet an fluid phases (second measurement)

8 Acknowledgements

The authors should like to acknowledge the support of the Forschungsvereinigung für Luft- und Trocknungstechnik e.V. which supported the experimental investigations by making available the measuring facility.